

Research Article

# Modeling of homogeneous tin speciation using detailed chemical kinetics<sup>†</sup>

Yu Qiao,<sup>1</sup> Minghou Xu,<sup>1\*</sup> Hong Yao,<sup>1</sup> Chen Wang,<sup>1</sup> Xun Gong,<sup>1</sup> Hanping Chen<sup>1</sup> and Laicai Li<sup>2</sup>

<sup>1</sup>State Key Laboratory of Coal Combustion, Huazhong University of Science and Technology, Wuhan 430074, China

<sup>2</sup>Department of Chemistry, Sichuan Normal University, Chengdu 610066, China

Received 20 July 2006; Revised 10 October 2006; Accepted 10 December 2006

**ABSTRACT:** In this work, *ab initio* molecular orbital methods were employed to study the reaction mechanisms of the oxidation of tin (Sn) with different oxidants, including O<sub>2</sub>, CO<sub>2</sub>, HOCl, HCl, ClO, ClO<sub>2</sub> and NO<sub>3</sub>, during coal combustion. Eleven key reaction pathways were identified. Although Cl<sub>2</sub> and HCl are generally low in concentration in coal and in the combustion flue gases, owing to their strong oxidizability, these oxidants should be considered for some trace element oxidation. A detailed kinetic modeling consisting of 354 reactions and 64 species especially for tin in combustion-generated flue gases was performed. The quantum chemistry and sensitivity simulations illustrated that the pathways Sn + O<sub>2</sub> = SnO + O and Sn + CO<sub>2</sub> = SnO + CO are more significant than the other nine reactions. The present study shows that O<sub>2</sub> and CO<sub>2</sub> are the two main oxidants for tin oxidation. © 2007 Curtin University of Technology and John Wiley & Sons, Ltd.

**KEYWORDS:** coal combustion; tin; chemical kinetics; quantum chemistry

## INTRODUCTION

Man has used tin since the Bronze Age. For thousands of years, tin and tin alloys have been used in the production of tin dishes or drinking mugs. Following the Industrial Revolution, inorganic tin compounds were produced for various purposes. Around 1940, the industrial production of organotin compounds started. Up to now, metallic tin, inorganic tin compounds and organotin compounds have been increasingly used in a variety of industrial and agricultural applications and have become a serious environmental threat. It is estimated that of the anthropogenic fluxes of tin in the environment may be as high as ten times its natural fluxes (Barbara *et al.*, 1997).

Some studies suggest that tin is a trace element essential for humans (possibly as an ionic constituent of gastrin, a stomach-stimulating peptide hormone). Natural foods contain trace amounts of tin. It is assumed that the average daily intake is in the range of 0.2–1 mg. However, organotin compounds have been proven to be related to toxicological effects. Triorganotin compounds are particularly toxic, which explains their wide use as

biocides (e.g. in antifouling paints or pesticides). The toxicity of different organotin compounds is related to the exposure concentration and duration, bioavailability and the sensitivity of organisms. Some organotins show specific toxic effects to different organisms even at very low concentrations.

Only a few ecotoxicological studies with metallic tin and inorganic tin compounds have been published. The provisional tolerable weekly intake for tin is 14 mg/kg body weight and the recommended maximum permissible levels of tin in food are typically 250 mg/kg (200 mg/kg in the UK) for solid foods and 150 mg/kg for beverages (MAFF, 1992). Adverse gastrointestinal effects have been observed in limited clinical studies at concentrations of 700 ppm or above. A food survey suggested that the contents of almost 4% of plain internal tinplate food cans contain over 150 mg/kg of tin, and over 2.5 million such cans are used every year in the UK alone (Steve and Tony, 2003). At the same time, a low toxicity of inorganic tin (Sn<sup>2+</sup>) was observed by Khangarot and Ray (1989).

Although the toxicity of metallic tin and inorganic tin compounds seems to be lower for some organotin compounds, it is assumed that under certain environmental conditions, methylation of inorganic tin by microorganisms takes place (Gadd, 2000). The occurrence of methyltin compounds in estuarine and coastal environments was monitored by Amouroux *et al.* (2000).

\*Correspondence to: Minghou Xu, State Key Laboratory of Coal Combustion, Huazhong University of Science and Technology, Wuhan 430074, China. E-mail: mhxu@mail.hust.edu.cn

<sup>†</sup>Presented at the 2006 Sino–Australia Symposium on Advanced Coal Utilization Technology, July 12–14, 2006, Wuhan, China.

In the past, some authors have doubted the occurrence of natural methylation of metallic tin and inorganic tin by microorganisms.

Coal combustion and tin processing industries are two main pollution sources of inorganic tin in air, soil, and waters. During the process of coal combustion, a part of the tin in coal, as well as mercury, arsenic, chromium and lead, may be emitted directly into the atmosphere. Additionally, tin would be partially condensed and adsorbed on the surface of fly ash particles as the temperature decreases in the stack flue. Some studies suggest that trace elements including tin are leachable in fly ash. The tin leaching result of fly ash from the Ptolemais coal-fired power plant (Northern Greece) was studied by Georgakopoulos *et al.* (2002). The interaction between tin and surface water and groundwater causes tin mobility into soil and waters: especially, since fly ash remains in the atmosphere for a long time. The emission of trace elements in air, soil, and waters has recently become a concern for the electric utility industry.

Tin exists mainly in the oxidation states of Sn(0), Sn(II), and Sn(IV). The states of tin in the fly ash affect the leachability because of the low water solubility of Sn(0) and the water-soluble oxidized species of Sn(II) and Sn(IV). In coal-fired plants, tin mainly exists in the state Sn(0) at high temperatures, and then Sn(0) gets oxidized to Sn(II). However, the effect of temperature on tin speciation is poorly understood. Thus, the speciation of tin in combustion stacks affects the capture of tin in air pollution control equipment. For example, water-soluble oxidized species, such as Sn(II) and Sn(IV), are more readily removed from the flue gases in scrubber systems. In aqueous solutions, Sn(IV) is more stable than Sn(II), which can be oxidized to Sn(IV).

Previous studies of tin oxidation in combustion systems have focused on chemical equilibrium calculations. It is well recognized that under the actual combustion conditions, tin oxidation would be kinetic-reaction controlled. Fontijn and Bajaj proposed the one-step global reaction mechanism of Sn(0) in the presence of O<sub>2</sub> and CO<sub>2</sub> (Fontijn and Bajaj, 1996). However, such mechanisms provide little insight into the details of the conversion process. To date, very little reliable kinetic rate data have been obtained for tin species in combustion systems and there is a need to verify these data. In the absence of actual rate data for the gas-phase reactions of tin, another approach to determine the rate constants is by the direct use of quantum chemistry and transition state theory. Quantum chemical calculation, which simulates the process of chemical reaction by a computer using theoretical systems of quantum mechanics, is the most accurate theoretical method for calculating energy and molecular geometry at present (Zheng *et al.*, 2005). However, a theoretical study of

tin kinetic mechanism has seldom been reported (Xu *et al.*, 2004).

The overall aim of this study is to look for different methods to prevent the pollutant Sn(0) from being emitted into the air. Attempts have been made to oxidize Sn(0) into soluble ions in a cooling process. By doing so, it is easier to be collected, which helps reduce air pollution. When Sn(0) is in the vapor phase, its low water solubility makes it difficult to be controlled. Our study mainly concentrated on the reaction mechanism and kinetics of stannic oxidation by potential oxidants (O<sub>2</sub>, CO<sub>2</sub>, HOCl, HCl, ClO, ClO<sub>2</sub> and NO<sub>3</sub>), and the further oxidation of SnO and SnCl by HOCl and HCl. Among these oxidants, O<sub>2</sub> and CO<sub>2</sub> are considered the two main components affecting tin oxidation (Fontijn and Bajaj, 1996). The purpose of this study is to provide guidelines for experimentalists, and to enrich the kinetic database in this area. Eleven elemental reactions of tin oxidation were investigated by *ab initio* calculations of quantum chemistry. The kinetic and thermodynamic parameters of these reactions were calculated to provide evidence for further research in the dynamic modeling of tin transformation and emission in coal combustion.

## SN(0) REACTION MECHANISM DEVELOPMENT

### Computational methodology

In this study, the kinetic mechanisms of the reactions were studied using *ab initio* calculations of quantum chemistry. The geometry configuration of the reactants, products, intermediates (M) and transition states (TS) were optimized at the MP2/SDD level. Here MP2 represents the Möller–Plesset energy correction, truncated at the second order and SDD is the basis function of the effective core potential (ECP). Vibrational frequency analyses were used to confirm the intermediates (M) and TS. The energy was calculated at the QCISD (T)/SDD level and corrected with zero-point energy. The rate constants were defined by the rate Eqn (1) according to the classic transition state theory (Belyung *et al.*, 1996).

$$k(T) = \lambda(k_B T/h)(Q^\ddagger/Q_A Q_B) \exp(-E_a/RT) \quad (1)$$

Here,  $\lambda$  is the correction factor for the quantum effect and generally set to unity,  $k_B$  is the Boltzman constant,  $Q^\ddagger$  is the partial function of the TSs,  $Q_A$  and  $Q_B$  are the partial functions of the reactants A and B,  $E_a$  is the activation energy,  $Q$  is the multiplier of the transitional ( $Q_t$ ), rotational ( $Q_r$ ) and vibrational ( $Q_v$ ) partial functions, which has the relationship  $Q = Q_t Q_r Q_v$ . The calculations were performed by employing the G98 programs (Frisch *et al.*, 1998).

## Reaction mechanism of the reactions

The following reactions are discussed in this paper:

1.  $\text{Sn} + \text{O}_2 \rightarrow \text{SnO} + \text{O}$
2.  $\text{Sn} + \text{CO}_2 \rightarrow \text{SnO} + \text{CO}$
3.  $\text{Sn} + \text{HOCl} \rightarrow \text{SnCl} + \text{OH}$
4.  $\text{Sn} + \text{HCl} \rightarrow \text{SnCl} + \text{H}$
5.  $\text{Sn} + \text{ClO} \rightarrow \text{SnO} + \text{Cl}$
6.  $\text{Sn} + \text{ClO}_2 \rightarrow \text{SnO} + \text{ClO}$
7.  $\text{Sn} + \text{NO}_3 \rightarrow \text{SnO} + \text{NO}_2$
8.  $\text{SnO} + \text{HCl} \rightarrow \text{SnCl} + \text{OH}$
9.  $\text{SnO} + \text{HOCl} \rightarrow \text{SnCl} + \text{HO}_2$
10.  $\text{SnCl} + \text{HCl} \rightarrow \text{SnCl}_2 + \text{H}$
11.  $\text{SnCl} + \text{HOCl} \rightarrow \text{SnCl}_2 + \text{OH}$

The studies by quantum chemistry show that

- Reaction (1) is a one-step reaction and there is no intermediate formed. During the reaction process, the distance between Sn and O reduces from 0.20551 nm to 0.1882 nm and the distance between O and O increases from 0.12241 nm to 0.139093 nm. The changes in the geometric configurations about the TS can clearly describe the process of the reaction. The optimized geometries of the reactants, products and the TS of reaction (1) are shown in Fig. 1.
- Reaction (2) is  $\text{Sn} + \text{CO}_2 \rightarrow \text{M1}(\text{SnOCO}) \rightarrow \text{TS1}(\text{SnOCO}) \rightarrow \text{M2}(\text{SnOCO}) \rightarrow \text{TS2}(\text{SnOCO}) \rightarrow \text{SnO} + \text{CO}$ . During the reaction process, the distance between Sn and O reduces gradually (0.34712 nm  $\rightarrow$  0.29579 nm  $\rightarrow$  0.25176 nm  $\rightarrow$  0.20714 nm  $\rightarrow$  0.1882 nm), and the distance between C and O increases gradually (0.12132 nm  $\rightarrow$  0.13102 nm  $\rightarrow$  0.20748 nm  $\rightarrow$  0.25619 nm  $\rightarrow$  0.35214 nm). The changes in the bond distance indicate the formation of the Sn–O bond and the breaking of the C–O bond. Here, TS means the TSs and M means an intermediate. The optimized geometries of reactants, products, TSs and intermediates of reaction (2) are shown in Fig. 2.
- Reaction (3) of Sn and HOCl is also a one-step reaction. The reactants form the products (SnCl and OH) directly through transition state TS3 (SnClOH) without any stable intermediate. During the reaction, the Sn atom gradually moves closer to the Cl atom. The distance between the two atoms is 0.3897 nm in TS3 and 0.2441 nm in the product SnCl; this means that it becomes short gradually and forms the Sn–Cl bond finally. Although the distance between the Cl

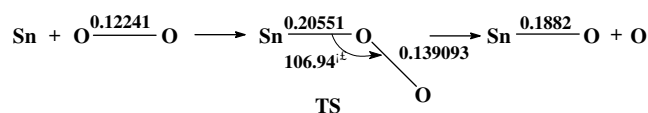


**Figure 1.** Reaction process of  $\text{Sn} + \text{O}_2 \rightarrow \text{SnO} + \text{O}$ .

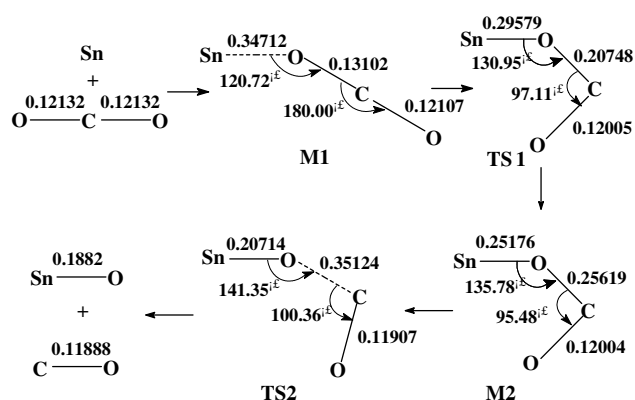


**Figure 2.** Reaction process of  $\text{Sn} + \text{CO}_2 \rightarrow \text{SnO} + \text{CO}$ .

and O atoms hardly changes during the process of the reactants to TS1, the Cl–O bond rapidly breaks after the formation of TS3 and produces SnCl and the OH radical. The geometric configuration of TS3 shows the reaction process distinctly.

- In reaction (4), Sn reacts with HCl to form the stable intermediate M3 (SnClH) through the transition state TS4 (SnClH), and then cleaves to produce SnCl and the H radical through another transition state TS5 (SnClH). It is a two-step reaction. The change of the distance between the Sn and the Cl atom is 0.3641  $\rightarrow$  0.3235  $\rightarrow$  0.2433 nm during the process of TS4  $\rightarrow$  M3  $\rightarrow$  TS5, which means that the Sn–Cl bond forms during the reaction process. The length of the H–Cl bond hardly changes in the process of  $\text{Sn} + \text{HCl} \rightarrow \text{TS4} \rightarrow \text{M3}$ , but lengthens gradually from 0.1284 nm in M1 to 0.1730 nm in TS3 and ultimately breaks.
- In reaction (5), the Sn atom approaches the O atom of the ClO radical to form the intermediate M4 (SnOCl) without a potential barrier. The length of the O–Cl bond increases from 0.1746 nm in M4(SnOCl) to 0.2263 nm in TS6 (SnOCl), and the O–Cl bond finally cleaves.
- In reaction (6), Sn attracts ClO<sub>2</sub> to form a stable intermediate M5 (SnOOC1), then decomposes into SnO and ClO through the transition state TS7 (SnOOC1). During the process of M5  $\rightarrow$  TS7, the Sn–O bond and O–O bond change from 0.2059 nm and 0.1435 nm in M5 to 0.1925 nm and 0.1801 nm in TS7, respectively.
- In reaction (7), Sn reacts with NO<sub>3</sub> to produce the stable intermediate M6 (SnONO<sub>2</sub>), and then decomposes into SnO and NO<sub>2</sub> through the transition state TS8 (SnONO<sub>2</sub>). During the process of M6  $\rightarrow$  TS8, the Sn–O bond and O–N bond change from 0.2318 nm and 0.1318 nm in M6 to 0.1987 nm and 0.1866 nm in TS8, respectively.
- In reaction (8), SnO approaches HCl to produce the stable intermediate M7(SnClOH) through the transition state TS9 (SnClOH), and then forms SnCl and

OH radicals through another transition state TS10 (SnClOH). During the process of TS9 → M7 → TS10, the Sn–Cl bond and the Sn–O bond change from 0.3197 nm and 0.1917 nm to 0.2456 nm and 0.1982 nm to 0.2551 nm and 0.3881 nm, respectively. These changes indicate that a Sn–Cl bond is formed.

- In reaction (9), HOCl is initially added to SnO to form stable intermediates M8 (SnClOOH) through the transition state TS11 (SnClOOH), followed by the production of SnCl and HO<sub>2</sub> radicals through the transition state TS12 (SnClOOH). It is also a two-step reaction. In the process of TS11 → M8 → TS12, the Sn–Cl bond and the O–O bond change from 0.2965 nm and 0.1842 nm to 0.2408 nm and 0.1458 nm to 0.2592 nm and 0.1299 nm, respectively.
- In reaction (10), SnCl reacts with HCl to produce the stable intermediate M9 (SnClClH), and then M9 decomposes into SnCl<sub>2</sub> and an H atom through the transition state TS13 (SnClClH).
- Finally, for reaction (11), an intermediate M10 (SnClClOH) is generated directly with a Sn–Cl bond length of 0.2522 nm. After this, the Cl–O bond lengthens from 0.1742 to 0.1960 nm and then cleaves to SnCl<sub>2</sub> and the OH radical.

In addition, all the intermediates have been identified as not having an imaginary frequency. The TSs have only one imaginary frequency by the vibration analysis, which further confirmed that they are the real compounds along the reaction pathways.

### Kinetic and thermodynamic parameters

According to the above studies on the reaction mechanisms and the optimized results, the reaction rate constants were calculated from the TS theory. The kinetic and thermodynamic parameters are tabulated in Table 1.

The reactions (4), (8) and (9), namely, Sn + HCl → TS4 → M3 → TS5 → SnCl + H, SnO + HCl → TS9 → M7 → TS10 → SnCl + OH and SnO + HOCl → TS11 → M8 → TS12 → SnCl + OOH, were completed in two steps. Only the barriers of the controlling steps for the three reactions are listed and considered in the rate constant calculations of the whole reactions. As for reaction (4), the barrier of the first step is 120.32 kJ/mol, and the barrier of the second step is 78.49 kJ/mol. So we calculated the rate constant of this reaction according to the barrier of the first step, which is the controlling step along the pathway. For reaction (8), the step SnO + HCl → TS9 → M7 has a high barrier of 285.70 kJ/mol, but the second step M7 → TS10 → SnCl + OH has a higher barrier of 393.81 kJ/mol. Thus, the second step is the controlling step and the reaction will take place with a very low rate. Similarly, with regard to reaction (9), the barrier of SnO + HOCl → TS11 → M8 (423.72 kJ/mol) is higher than that of M8 → TS12 → SnCl + OOH (271.69 kJ/mol), so the rate constant of reaction (9) is found according to the first step. From the parameters in Table 1, we can see that the reactions (3), (5), (8) and (9) have high barriers, so the four reactions would happen with very small probabilities. On the contrary, the barriers of the reaction (10) and (11) are only 31.12 kJ/mol and 87.68 kJ/mol, respectively. They are both fast reaction pathways.

According to the rate constants *k* listed in Table 1, we can further discuss the 11 reactions. The rate constants of the reactions (1)–(7), namely, of the reactions Sn (0) with CO<sub>2</sub>, O<sub>2</sub>, HOCl, HCl, OCl, ClO<sub>2</sub> and NO<sub>3</sub>, are  $7.28 \times 10^{-11}$ ,  $3.68 \times 10^{-13}$ ,  $1.90 \times 10^{-54}$ ,  $1.92 \times 10^{-12}$ ,  $1.97 \times 10^{-33}$ ,  $7.76 \times 10^{-14}$  and  $3.00 \times 10^{-16}$ , respectively. The reactions of Sn(0) with HOCl and OCl are of low probability to take place. However, Sn can readily react with CO<sub>2</sub>, O<sub>2</sub>, HCl, ClO<sub>2</sub> and NO<sub>3</sub> with larger rate constants. As for the reactions (8) and (9), they both have very small rate constants,  $1.51 \times 10^{-55}$  and  $1.59 \times 10^{-69}$ ; therefore they

**Table 1. Kinetic and thermodynamic parameters of Sn reactions in coal combustion flue gas.**

Reaction	$E_a$ (kJ/mol)	$\Delta H$ (kJ/mol)	$\Delta S$ (kcal/mol)	$k(T = 298 \text{ K})$
(1)	2.97	93.05	2.314E-3	$7.28 \times 10^{-11}$
(2)	72.71	431.62	6.741E-2	$3.68 \times 10^{-13}$
(3)	363.31	114.93	4.41	$1.90 \times 10^{-54}$
(4)	120.32	-43.35	1.16	$1.92 \times 10^{-12}$
(5)	271.51	508.83	0.51	$1.97 \times 10^{-33}$
(6)	157.00	447.27	2.76	$7.76 \times 10^{-14}$
(7)	160.21	811.53	4.89	$3.00 \times 10^{-16}$
(8)	393.81	-251.47	3.09	$1.51 \times 10^{-55}$
(9)	423.72	-216.16	3.21	$1.59 \times 10^{-69}$
(10)	31.12	-19.29	-4.59	$3.92 \times 10^7$
(11)	87.68	411.69	-2.44	$6.05 \times 10^{-3}$

can hardly take place. This means that SnO can hardly be converted into SnCl by HOCl and HCl. On the other hand, SnCl may be further oxidized into SnCl<sub>2</sub> by HOCl and HCl freely because of their large rate constants,  $3.92 \times 10^7$  and  $6.05 \times 10^{-3}$ , respectively.

### Solution procedure

The present kinetic calculations are based on the package CHEMKIN-3.7 (Kee *et al.*, 1996). The rate coefficients are in the modified Arrhenius form,  $k = AT^\beta \exp(-E_a/RT)$ . The external factors considered to be involved are temperatures from 400–1800 K and a constant pressure of 1.0 atm. In this work, other supporting submechanisms were taken directly from the literature (Roesler *et al.*, 1992; 1995; Allen *et al.*, 1997; Mueller *et al.*, 1999a,b, 2000), and the GRI-Mech 3.0 database was used without modification excluding the 11 key reactions from the quantum chemistry calculation results. Thermodynamic curve fits for Sn compounds and some Cl compounds were obtained from the National Institute of Standards and Technology chemical species database (Mallard *et al.*, 1998), while information for the other species was obtained from the GRI-Mech 3.0 database. In total, 354 elementary reactions and 64 species were included in the present kinetic model.

## RESULTS AND DISCUSSION

### Kinetic modeling of simulation of the flue gas

In order to assess the reaction chemistry of tin under conditions typically encountered in coal combustion facilities, a bench-scale experimental study of tin oxidation in the presence of different reaction species is essential. Unfortunately, such an experimental study has not been reported. In the present work, the concentrations of the three cases used for the kinetic

calculation were initialized, the typical concentration ranges taken according to some experiments in mercury oxidation. In those experimental systems, a methane-fuelled flat flame burner facility was used to generate 800–1500 K postcombustion gases containing different oxidants (Sliger *et al.*, 1998; Mamani-Paco and Herble, 2000; Widmer and West, 2000). The concentrations of Cl<sub>2</sub> or HCl were higher than that of industrial-scale coal combustors in studying their influence on mercury oxidation. The oxidants Cl<sub>2</sub> and HCl cannot be neglected in trace element oxidation because of their strong oxidizability, although they are usually low in concentrations in coal and the flue gas. On the other hand, concentration range of tin found in different American coals ranges from 1 to 400 ppm (Linak and Wendt, 1993). Additionally, there is a wide concentration range of tin during the postcombustion. In fact, through the kinetic simulation it was found that the effect of the initial concentration of tin could be neglected when O<sub>2</sub> and CO<sub>2</sub> were both abundant. In any case, the concentration of tin was less than that of O<sub>2</sub> and CO<sub>2</sub> in the flue gas. In this work, 10 ppm of tin concentration was used for the kinetic simulation. The initial compositions of tin and the flue gas used for kinetic calculation are shown in Table 2.

### Influence of compositions and temperature

Figure 3 shows the temporal concentration of SnO under three compositions and at temperatures 1000 and 1500 K. As shown in Fig. 3, the Sn(0) was oxidized rapidly to SnO, and 99% SnO was observed in approximately 0.5 s when the CO<sub>2</sub> and O<sub>2</sub> were both abundant at temperature 1500 K. When only CO<sub>2</sub> was abundant at a temperature 1500 K, the formation rate of SnO was evidently slower. If the residence time were extended to 10 s, about 99% oxidation would be obtained. At a lower temperature (1000 K), 30% SnO was observed in approximately 0.5 s when the CO<sub>2</sub> and O<sub>2</sub> were both abundant. When only CO<sub>2</sub> is abundant at a temperature of 1000 K, the formation rate of SnO is very slow.

**Table 2. Compositions for kinetic simulation.**

Species	Composition (mole fraction)		
	10 ppm		
Sn(0)	Case 1	Case 2	Case 3
Flue gas	(Mamani-Paco and Herble, 2000)	(Widmer and West, 2000)	(Sliger <i>et al.</i> , 1998)
O <sub>2</sub>	0.0	0.10	0.0743
CO <sub>2</sub>	0.13	0.10	0.0615
H <sub>2</sub> O	0.26	0.08	0.123
Cl <sub>2</sub>	Varied as indicated	Not defined	Not defined
HCl	Not defined	$300 \times 10^{-6}$ , $3000 \times 10^{-6}$	Varied as indicated
N <sub>2</sub>	Balance	Balance	Balance

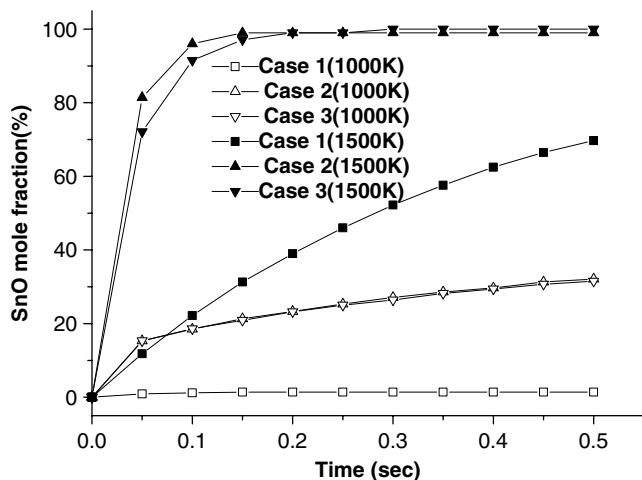


**Figure 3.** SnO temporal concentrations of kinetic simulation under three compositions.

Only 1.5% SnO was obtained in approximately 0.5 s, and tin mainly existed in the state Sn(0). In the reaction process of three cases, very little SnCl<sub>2</sub> or SnCl was observed, regardless of the temperature. It seems impossible that Sn(0) could be oxidized to SnCl<sub>2</sub> under those reaction conditions. The kinetic calculation results show that the oxidants of Cl<sub>2</sub> and HCl have no significant influence on tin oxidation because of their low concentrations in postcombustion flue gases, although some reactions involving HCl and ClO<sub>2</sub> also have large rate constants as shown by quantum chemical analyses (shown in Table 1).

### Sensitivity analysis

The applications of the sensitivity analysis in combustion chemistry are usually related to either the large size and complexity of combustion models or the high uncertainty of their parameters. In order to further discuss the above kinetic results, SENKIN sensitivity analyses are presented. A sensitivity analysis usually identifies the rate-limiting step of the mechanism under certain reaction conditions. In Figs 4, 5 and 6, the three cases of sensitivity of Sn(0) concentrations towards the dominant reaction rates are shown as a function of time. For the flue gas composition in Case 1 (at a temperature 1500 K), it can be seen from Fig. 4 that only the reaction  $\text{Sn} + \text{CO}_2 = \text{SnO} + \text{CO}$  has been identified as the dominant reaction in Sn production among the reactions listed in Table 1. This suggests that among all the reactions involving SnO, SnCl and SnCl<sub>2</sub> in this work, the reaction  $\text{Sn} + \text{CO}_2 = \text{SnO} + \text{CO}$  is the dominant reaction in the production of Sn, while others are relatively less significant.

Figures 5 and 6 present the sensitivity derivatives as a function of time for Case 2 and Case 3 at a temperature

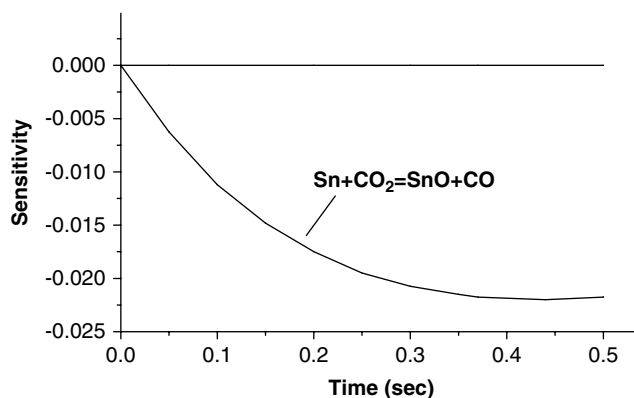


**Figure 4.** Sn(0) sensitivity derivatives vs time seen in simulations of Case 1 at 1500 K.

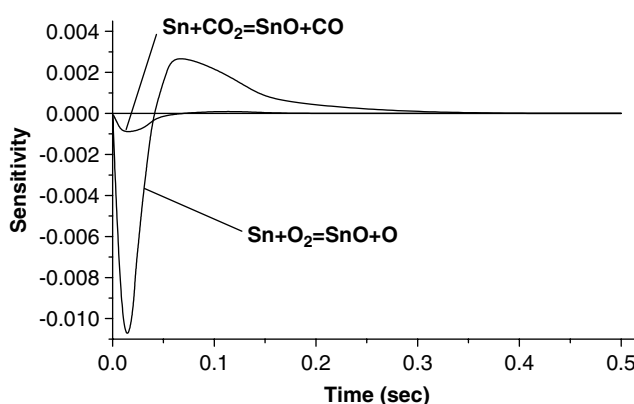


**Figure 5.** Sn(0) sensitivity derivatives vs time seen in simulations of Case 2 at 1500 K.

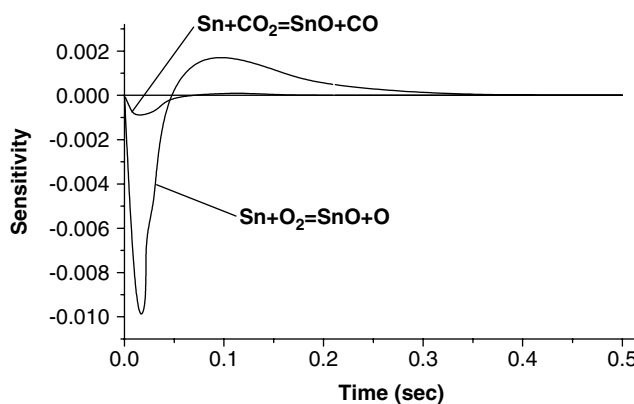


**Figure 6.** Sn(0) sensitivity derivatives vs time seen in simulations of Case 3 at 1500 K.

1500 K. Similar results are shown in the presence of abundant oxidants O<sub>2</sub> and CO<sub>2</sub>. Sn(0) concentrations are more sensitive to the rate coefficients of the reactions  $\text{Sn} + \text{O}_2 = \text{SnO} + \text{O}$  and  $\text{Sn} + \text{CO}_2 = \text{SnO} + \text{CO}$  than those of other nine reactions. From these two figures, it can be confirmed that the dominant reaction is Sn +

$O_2 = SnO + O$  when  $O_2$  and  $CO_2$  are both abundant. The above results explain why the concentration of SnO increases slowly when there is no oxidant  $O_2$  for tin oxidation. It also shows that the oxidants  $Cl_2$  and HCl have no significant influence on tin oxidation because of their low concentrations during the coal postcombustion process.

## CONCLUSIONS

A detailed chemical kinetic model to simulate tin speciation in the flue gas was developed. This speciation model includes potential oxidants  $CO_2$ ,  $O_2$ , HOCl, HCl, ClO,  $ClO_2$  and  $NO_3$ , which are important flue gas components, as well as 11 tin oxidation pathways with new reaction rate constants calculated directly from quantum chemistry. Analyses by quantum chemistry and sensitivity simulations illustrated that the pathways  $Sn + O_2 = SnO + O$  and  $Sn + CO_2 = SnO + CO$  are more significant than the other nine reactions. The studies on the effects of oxidants show that  $O_2$  and  $CO_2$  promote tin oxidation, especially under the condition of 1500 K temperature, which is consistent with the literature reported. Although the present results do not include the data from a bench-scale experimental study, it has provided a useful guide for experimentalists and enriched the kinetic database in this area.

## Acknowledgements

This work was supported by National Natural Science Foundation of China (90610017, 50325621, 20277014). Partial support by the Programme of Introducing Talents of Discipline to Universities ('111' project No. B06019), China, and the Natural Science Foundation of the Hubei Province (2006ABC002) is also acknowledged.

## REFERENCES

- Allen MT, Yetter RA, Dryer FL. High pressure studies of moist carbon monoxide/nitrous oxide kinetics. *Combust. Flame* 1997; **109**: 449–470.
- Amouroux D, Tessier E, Donard OFX. Volatilization of organotin compounds from estuarine and coastal environments. *Environ. Sci. Technol.* 2000; **34**: 988–995.
- Barbara P, Renata K, Tadeusz S. The impact of inorganic tin on the planktonic cyanobacterium *synechocystis aquatilis*; the effect of pH and humic acid. *Environ. Pollut.* 1997; **97**(1–2): 65–69.
- Belyung DP, Hranisaoljevic J, Kashireniov O, Santana GM, Fontijn A, Marshall P. Laser-induced fluorescence and mass spectrometric studies of the CU HCl reaction over a wide temperature range. *J. Phys. Chem.* 1996; **100**: 17835.
- Fontijn A, Bajaj PN. Kinetics of the SN(3PO) reactions with  $CO_2$  and  $O_2$  over wide temperature ranges. *J. Phys. Chem.* 1996; **100**: 7085–7089.
- Frisch MJ, Trucks GW, Schlegel HB, Scuseria GE, Robb MA, Cheeseman JR, Zakrzewski VG, Montgomery JA, Stratmann RE, Burant JC. *Gaussian 98 Rev. A4*. Gaussian: Pittsburgh, PA, 1998.
- Gadd GM. Microbial interactions with tributyltin compounds; detoxification, accumulation, and environmental fate. *Sci. Total Environ.* 2000; **258**: 119–127.
- Georgakopoulos A, Filippidis A, Kassoli A, Fernandez-Turiel JL, Llorens JF, Mousty F. Leachability of major and trace elements of fly ash from Ptolemais Power Station, Northern Greece. *Energy Sources* 2002; **24**: 103–113.
- Kee RJ, Ruply FM, Meeks E, Miller JA. CHEMKIN- $\epsilon$ : A Fortran chemical kinetics package for the analysis of gas phase chemical kinetics. SAND96-8216, 1996.
- Khargarot BS, Ray P. Investigation of correlation between physiochemical properties of metals and their toxicity to the water flea, *Daphnia magna*, Straus. *Ecotoxicol. Environ. Saf.* 1989; **18**: 109–120.
- Linak WP, Wendt JOL. Toxic metal emissions from incineration mechanisms and control. *Prog. Energy Combust. Sci.* 1993; **19**: 145–185.
- MAFF. The tin in food regulations. S.I. 496. *UK Ministry of Agriculture, Fisheries and Food*. HMSO: London, 1992.
- Mallard WG, Westley F, Herron JT, Hampson RF, Frizzell DH. NIST Chemical Kinetic Database, 1998.
- Mamani-Paco RM, Herble JJ. Bench-scale examination of mercury oxidation under non-isothermal conditions. In *93rd Annual Meeting, Air & Waste Management Association.*, Salt Lake City, Utah, 2000.
- Mueller MA, Yetter RA, Dryer FL. Flow reactor studies and kinetic modeling of the  $H_2/O_2$  reaction. *Int. J. Chem. Kinet.* 1999a; **31**: 113–125.
- Mueller MA, Yetter RA, Dryer FL. Flow reactor studies and kinetic modeling of the  $H_2/O_2/NO_x$  and  $CO/H_2O/O_2/NO_x$  reactions. *Int. J. Chem. Kinet.* 1999b; **31**: 705–724.
- Mueller MA, Yetter RA, Dryer FL. Kinetic modeling of the  $CO/H_2O/O_2/NO/SO_2$  system: Implications for high-pressure fall-off in the  $SO_2 + O(+M) = SO_3(+M)$  reaction. *Int. J. Chem. Kinet.* 2000; **32**: 317–339.
- Roesler JF, Yetter RA, Dryer FL. Detailed kinetic modeling of moist CO oxidation inhibited by trace quantities of HCl. *Combust. Sci. Technol.* 1992; **85**: 1–22.
- Roesler JF, Yetter RA, Dryer FL. Kinetic interactions of CO,  $NO_x$  and HCl emissions in postcombustion gases. *Combust. Flame* 1995; **100**: 495–504.
- Sliger NR, Going JD, Kramlich JC. *Kinetic Investigation of the High-temperature Oxidation of Mercury by Chlorine Species*. Western State Section/The Combustion Institute, Fall Meeting: Seattle, WA, 1998.
- Steve B, Tony W. Tin in canned food: a review and understanding of occurrence and effect. *Food Chem. Toxicol.* 2003; **41**: 1651–1662.
- Widmer NC, West J. Thermochemical study of mercury oxidation in utility boiler fuel gases. In *93rd Annual Meeting, Air & Waste Management Association.*, Salt Lake City, Utah, 2000.
- Xu M, Li L, Tian A. A kinetic study on tin oxidation. In *21st Annual International Pittsburgh Coal Conference.*, Osaka, Japan, Sep 13–17, 2004.
- Zheng C, Liu J, Liu Z, Xu M, Liu Y. Kinetic mechanism studies on reactions of mercury and oxidizing species in coal combustion. *Fuel* 2005; **84**(10): 1215–1220.